Pruning has a disparate impact on model accuracy

Cuong Tran
Department of Computer Science
Syracuse University
cutran@syr.edu

Ferdinando Fioretto
Department of Computer Science
Syracuse University
ffiorett@syr.edu

Jung-Eun Kim
Department of Computer Science
Syracuse University
jkim150@syr.edu

Rakshit Naidu
Department of Computer Science
Carnegie Mellon University
rnemakal@andrew.cmu.edu

Abstract

Network pruning is a widely-used compression technique that is able to significantly scale down overparameterized models with minimal loss of accuracy. This paper shows that pruning may create or exacerbate disparate impacts. The paper sheds light on the factors to cause such disparities, suggesting differences in gradient norms and distance to decision boundary across groups to be responsible for this critical issue. It analyzes these factors in detail, providing both theoretical and empirical support, and proposes a simple, yet effective, solution that mitigates the disparate impacts caused by pruning.

1 Introduction

As deep learning models evolve and become more powerful, they also become larger and more costly to store and execute. The trend hinders their deployment in resource-constrained platforms, such as embedded systems or edge devices, which require efficient models in time and space. To address this challenge, studies have developed a variety of techniques to prune the relatively insignificant or insensitive parameters from a neural network while ensuring competitive accuracy [1, 5, 7, 29, 30, 31, 40]. When a model needs to be developed to fit given and certain requirements in size and resource consumption, a pruned model which is derived from a large, rigorously-trained, and (often) over-parameterized model, is regarded as a de-facto standard. That is because it performs incomparably better than a same-size dense model which is trained from scratch, when the same amount of effort and resources are invested.

In spite of its strengths, pruning has been showed to induce or exacerbate disparate effects in the accuracy of the resulting reduced models [19, 18]. Intuitively, the removal of model weights affects the process in which the network separates different classes, which can have contrasting consequences for different groups of individuals. This paper further shows that the accuracy of the pruned models tends to increase (decrease) more in classes that had already high (low) accuracy in the original model, leading to a "the rich get richer" and "the poor get poorer" effect. This *Matthew* effect is illustrated in Figure 1. The figure shows the accuracy of a facial recognition task on different demographic groups for several pruning rates (indicating the percentage of parameters removed from the original models). Notice how the accuracy of the majority group (White) tends to increase while that of the minority groups tends to decrease as the pruning ratio increases.

Following these observations, the paper sheds light on the factors to cause such disparities. The theoretical findings suggest the presence of two key factors responsible for why accuracy disparities arise in pruned models: **(1)** disparity in *gradient norms* across groups, and **(2)** disparity in *Hessian*
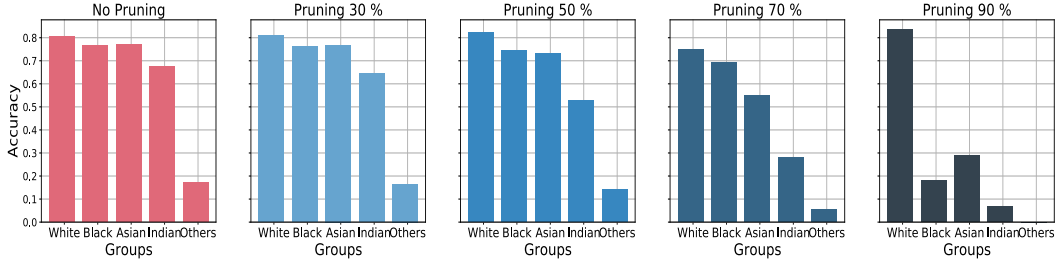
Figure 1: Accuracy of each demographic group in the UTK-Face dataset using Resnet18 [17], at the increasing of the pruning rate.

matrices associated with the loss function computed using a group's data. Informally, the former carries information about the groups' local optimality, while the latter relates to model separability. The paper analyzes these factors in detail, providing both theoretical and empirical support on a variety of settings, networks, and datasets.

By recognizing these factors, the paper also develops a simple yet effective training technique that largely mitigates the disparate impacts caused by pruning. The method is based on an alteration of the loss function to include components that penalize disparity of the average gradient norms and distance to decision boundary across groups.

These findings are significant: *Pruning is a key enabler for neural network models in embedded systems with deployments in security cameras and sensors for autonomous devices for applications where fairness is an essential need. (e.g., face recognition), Without careful consideration of the fairness impact of these techniques, the resulting models can have profound effects on our society and economy.*

Related work

Fairness and network pruning have been long studied in isolation. The reader is referred to the related papers and surveys on fairness [4, 8, 11, 16, 23] and pruning [1, 5, 7, 29, 30, 31, 32, 40] for a review on these areas.

The recent interest in assessing societal values of machine learning models has seen an increase of studies at the intersection of different properties of a learning model and their effects on fairness. For example, Xu et al. [38] studies the setting of adversarial robustness and show that adversarial training introduces unfair outcomes in term of accuracy parity [41]. Zhu et al. [43] show that semisupervised settings can introduce unfair outcomes in the resulting accuracy of the learned models. Finally, several authors have also shown that private training can have unintended disparate impacts to the resulting models' outputs [3, 13, 33, 35, 42] and downstream decisions [28, 34].

Network compression has also been shown to have a profound impact towards the model fairness. For example, several works observed empirically that network compression may amplify unfairness in different learning tasks [26, 18, 19, 21]. Most of the focus has been on vision tasks and in identifying the set of *Pruning Identified Exemplars* (PIEs), the samples that are impacted most under the compression scheme and conclude that PIEs belongs to low frequency groups (those observed at the tail of the data distribution). Blakeney et al. [6] further investigate how bias could be evaluated and mitigated in pruned neural networks using knowledge distillation while Hosseini et al. [20] observed empirically that knowledge distillation processes may produce unfair student models. The impact of network compression towards fairness has also been assessed in natural language tasks. For example, Du et al. [10] and Xu et al. [36] empirically measure the robustness of compressed large language models, while Ahia et al. [2] look into how compression schemes affects data-limited regimes. Finally, Xu and Hu [37] investigate ways to improve fairness in generative language models by compressing them.

This paper builds on this body of work and their important empirical observations and provides a step towards a deeper theoretical understanding of the fairness issues arising as a result of pruning. It derives conditions and studies the causes of unfairness in the context of pruning as well as it introduces mitigating guidelines.

2 Problem settings and goals

The paper considers datasets D consisting of n datapoints $(\boldsymbol{x}_i, a_i, y_i)$, with $i \in [n]$, drawn i.i.d. from an unknown distribution Π. Therein, $\boldsymbol{x}_i \in \mathcal{X}$ is a feature vector, $a_i \in \mathcal{A}$ with $\mathcal{A} = [m]$ (for some finite m) is a demographic group attribute, and $y_i \in \mathcal{Y}$ is a class label. For example, consider the case of a face recognition task. The training example feature $\boldsymbol{x}_i$ may describe a headshot of an individual, the protected attribute a_i may describe the individual's gender or ethnicity, and y_i represents the identity of the individual. The goal is to learn a predictor $f_{\boldsymbol{\theta}} : \mathcal{X} \to \mathcal{Y}$, where $\boldsymbol{\theta}$ is a k-dimensional real-valued vector of parameters that minimizes the empirical risk function:

$$\overset{\star}{\boldsymbol{\theta}} = \underset{\boldsymbol{\theta}}{\operatorname{argmin}} \, J(\boldsymbol{\theta}; D) = \frac{1}{n} \sum_{i=1}^{n} \ell(f_{\boldsymbol{\theta}}(\boldsymbol{x}_i), y_i), \tag{1}$$

where $\ell : \mathcal{Y} \times \mathcal{Y} \to \mathbb{R}_+$ is a non-negative *loss function* that measures the model quality.

The paper focuses on analyzing properties arising when extracting a small model $f_{\bar{\boldsymbol{\theta}}}$ with $\bar{\boldsymbol{\theta}} \subset \overset{\star}{\boldsymbol{\theta}}$ of size $|\bar{\boldsymbol{\theta}}| = \bar{k} \ll k$. Model $f_{\bar{\boldsymbol{\theta}}}$ is constructed by pruning the least important values or filters from vector $\overset{\star}{\boldsymbol{\theta}}$ (i.e., those with smaller values in magnitude) according to a prescribed criterion, such as an ℓ_p norm [24, 30]. The paper focuses on understanding the fairness impacts (as defined next) arising when pruning general classifiers, such as neural networks.

Fairness The fairness analysis focuses on the notion of *excessive loss*, defined as the difference between the original and the pruned risk functions over some group $a \in \mathcal{A}$:

$$R(a) = J(\bar{\boldsymbol{\theta}}; D_a) - J(\overset{\star}{\boldsymbol{\theta}}; D_a), \tag{2}$$

where D_a denotes the subset of the dataset D containing samples $(\boldsymbol{x}_i, a_i, y_i)$ whose group membership $a_i = a$. Intuitively, the excessive loss represents the change in loss (and thus, in accuracy) that a given group experiences as a result of pruning. Fairness is measured in terms of the maximal *excessive loss difference*, also referred to as *fairness violation*:

$$\xi(D) = \max_{a,a' \in \mathcal{A}} |R(a) - R(a')|, \tag{3}$$

defining the largest excessive loss difference across all protected groups. (Pure) fairness is achieved when $\xi(D) = 0$, and thus a fair pruning method aims at minimizing the excessive loss difference.

The goal of this paper is to shed light on why fairness issues arise (i.e., $R(a) > 0$) as a result of pruning, why some groups suffer more than others (i.e., $R(a) > R(a')$), and what mitigation measures could be taken to minimize unfairness due to pruning.

The paper uses the following notation: variables are denoted by calligraph symbols, vectors or matrices by bold symbols, and sets by uppercase symbols. Finally, $\| \cdot \|$ denotes the Euclidean norm and the paper uses $f_{\boldsymbol{\theta}}(\boldsymbol{x})$ to refer to the model' *soft* outputs. All proofs are reported in Appendix A.

3 Fairness analysis in pruning: Roadmap

To gain insights on how pruning may introduce unfairness, the paper starts with providing a useful upper bound for a group's excessive loss. Its goal is to isolate key aspects of model pruning that are responsible for the observed unfairness. The following discussion assumes the loss function $\ell(\cdot)$ to be at least twice differentiable, which is the case for common ML loss functions, such as mean squared error or cross entropy loss.

Theorem 1. *The excessive loss of a group $a \in \mathcal{A}$ is upper bounded by[1]:*

$$R(a) \leq \left\| \boldsymbol{g}_a^{\ell} \right\| \times \left\| \bar{\boldsymbol{\theta}} - \overset{\star}{\boldsymbol{\theta}} \right\| + \frac{1}{2} \lambda \left(\boldsymbol{H}_a^{\ell} \right) \times \left\| \bar{\boldsymbol{\theta}} - \overset{\star}{\boldsymbol{\theta}} \right\|^2 + O \left(\left\| \bar{\boldsymbol{\theta}} - \overset{\star}{\boldsymbol{\theta}} \right\|^3 \right), \tag{4}$$

where $\boldsymbol{g}_a^{\ell} = \nabla_{\boldsymbol{\theta}} J(\overset{\star}{\boldsymbol{\theta}}; D_a)$ is the vector of gradients associated with the loss function ℓ evaluated at $\overset{\star}{\boldsymbol{\theta}}$ and computed using group data D_a, $\boldsymbol{H}_a^{\ell} = \nabla_{\boldsymbol{\theta}}^2 J(\overset{\star}{\boldsymbol{\theta}}; D_a)$ is the Hessian matrix of the loss function ℓ, at the optimal parameters vector $\overset{\star}{\boldsymbol{\theta}}$, computed using the group data D_a (henceforth simply referred to as group hessian), and $\lambda(\Sigma)$ is the maximum eigenvalue of a matrix Σ.

---

[1]With a slight abuse of notation, the results refer to $\bar{\boldsymbol{\theta}}$ as the homonymous vector which is extended with $k - \bar{k}$ zeros.

The bound above follows from a second order Taylor expansion of the loss function, Cauchy-Schwarz inequality, and properties of the Rayleigh quotient.

Notice that, in addition to the difference in the original and pruned parameters vectors, two key terms appear in Equation (9): **(1)** The norms of the gradients g_a^ℓ and **(2)** the maximum eigenvalue of the Hessian matrix H_a^ℓ for a group a. Informally, the former is associated with the groups' local optimality while the latter relates to the ability of the model to separate the groups data. As we will show next these components represent the main sources of unfairness due to model pruning.

The following is an important corollary of Theorem 1. It shows that the larger the pruning, the larger will be the excessive loss for a given group.

Corollary 1. *Let $\bar{k}$ and $\bar{k}'$ be the size of parameter vectors $\bar{\theta}$ and $\bar{\theta}'$, respectively, resulting from pruning model $f_{\hat{\theta}}^\star$, where $\bar{k} < \bar{k}'$ (i.e., the former model prunes more weight than the latter one). Then, for any group $a \in \mathcal{A}$,*

$$\tilde{R}(a, \bar{\theta}) \geq \tilde{R}(a, \bar{\theta}'), \tag{5}$$

where $\tilde{R}(a, \omega)$ is the excessive loss upper bound computed using pruned model parameters ω (Eq. (9)).

A consequence of the corollary above is that as the pruning regime increases, the unfairness in accuracy across groups may also become more significant, which the paper shows next.

The next sections analyze the effect of gradient norms and the Hessian to unfairness in the pruned models. The theoretical claims are supported and complemented by analytical results. These results use the UTKFace dataset [39] for a vision task whose goal is to classify ethnicity. The experiments use a ResNet-18 architecture and the pruning counterparts remove the *P%* parameters with the smallest absolute values for various *P*. All reported metrics are normalized and an average of 10 repetitions. While the theoretical analysis focuses on the notion of disparate impacts under the lens of excessive loss, the empirical results report differences in accuracy of the resulting models. The empirical results thus reflect the setting commonly adopted when measuring accuracy parity [41].

The paper reports a glimpse of the empirical results, with the purpose of supporting the theoretical claims, and extended experiments, as well as additional descriptions of the datasets and settings, are reported in Appendix C and C.

4   Why disparity in groups' gradients causes unfairness?

This section analyzes the effect of gradients norms on the unfairness observed in the pruned models. In more detail, it shows that unbalanced datasets result in a model with large differences in gradient norms between groups (Proposition 1), it connects gradients norms for a group with the resulting model errors in such a group (Proposition 2), and connects these concepts with the excessive loss (Theorem 1) to show that unfairness in model pruning is largely controlled by the difference in gradient norms among groups.

Gradient norms and group sizes.   The section first shows that imbalanced datasets lead a model to have imbalanced gradient norms across groups. The following result assumes that the training converges to a local minima.

Proposition 1. *Consider two groups a and b in $\mathcal{A}$ with $|D_a| \geq |D_b|$. Then $\left\| g_a^\ell \right\| \leq \left\| g_b^\ell \right\|$.*

That is, groups with more data samples will result in smaller gradients norms than groups with fewer data samples and vice-versa. Figure 2 illustrates Proposition 1. The plot shows the relation between groups sizes $|D_a|$ and their associated gradient norms $\|g_a^\ell\|$ on the UTK dataset and settings described above. Notice the strong trend between decreasing group sizes and increasing gradient norms for such groups.
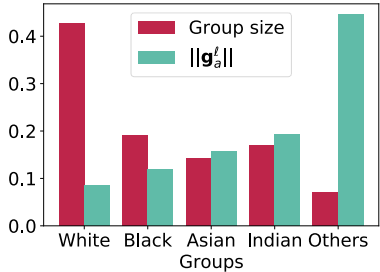

Figure 2: Group size vs. gradient norms.

Gradient norms and accuracy.   Next, the section shows a strong connection between the gradient norms of a group and its associated accuracy. The following assumes the models adopt a cross entropy loss (or mean squared error for regression tasks, as shown Appendix A).

4

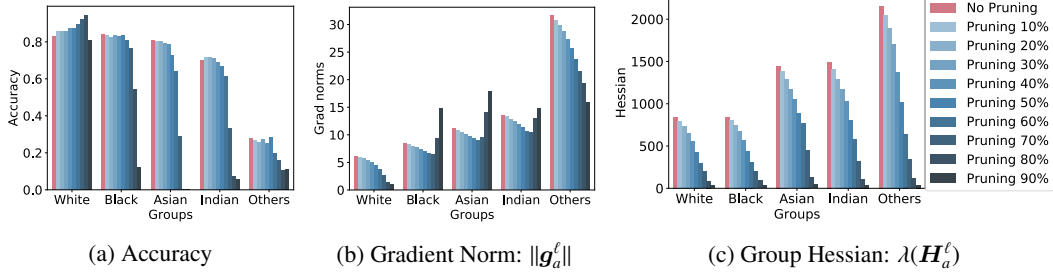(a) Accuracy   (b) Gradient Norm: $\|g_a^\ell\|$ (c) Group Hessian: $\lambda(H_a^\ell)$

Figure 4: Accuracy, gradient norm, and group Hessian max eigenvalues of each ethnicity group, before and after increasing pruning ratios for UTK-Face dataset. The percentage of data samples across groups *White, Black, Asian, Indian, and Others* is $\sim 0.42, 0.19, 0.15, 0.15, 0.07$, respectively.

Proposition 2. *For a given group $a \in \mathcal{A}$, gradient norms can be upper bounded as:*

$$\|g_a^\ell\| \in O\left(\sum_{(\boldsymbol{x},y)\in D_a} \underbrace{\|f_{\hat{\boldsymbol{\theta}}}(\boldsymbol{x}) - y\|}_{Accuracy} \times \left\|\nabla_{\boldsymbol{\theta}} f_{\boldsymbol{\theta}}^\star(\boldsymbol{x})\right\| \right).$$

The above relates gradient norms with an error measure of the classifier to a target label multiplied by the gradient of the predictions. For example, in a classification task with cross entropy loss, $\ell(f_{\boldsymbol{\theta}}(\boldsymbol{x}), y) = - \sum_{z\in\mathcal{Y}} f_{\boldsymbol{\theta}}^z(\boldsymbol{x})\boldsymbol{y}^z$, where $f_{\boldsymbol{\theta}}^z(\boldsymbol{x})$ represents the z-th element of the output associated with the soft-max layer of model $f_{\boldsymbol{\theta}}$, and $\boldsymbol{y}$ is a one-hot encoding of the true label y, with $\boldsymbol{y}^z$ representing its z-th element, then,

$$\|g_a\| = \|\nabla_{\boldsymbol{\theta}} J(\boldsymbol{\theta}; D_a,)\| = \left\| 1/|D_a| \sum_{(\boldsymbol{x},y)\in D_a} \nabla_f \ell(f_{\boldsymbol{\theta}}(\boldsymbol{x}), y) \times \nabla_{\boldsymbol{\theta}} f_{\boldsymbol{\theta}}(\boldsymbol{x}) \right\|$$

$$= \left\| 1/|D_a| \sum_{(\boldsymbol{x},y)\in D_a} (f_{\boldsymbol{\theta}}(\boldsymbol{x}) - \boldsymbol{y}) \times \nabla_{\boldsymbol{\theta}} f_{\boldsymbol{\theta}}(\boldsymbol{x}) \right\|$$

$$\leq 1/|D_a| \sum_{(\boldsymbol{x},y)\in D_a} \|f_{\boldsymbol{\theta}}(\boldsymbol{x}) - \boldsymbol{y}\| \times \|\nabla_{\boldsymbol{\theta}} f_{\boldsymbol{\theta}}(\boldsymbol{x})\|.$$

Figure 3: Accuracy vs. gradient norms.

A similar observation holds for mean square error loss, as illustrated in Appendix A. The observation above sheds light on the correlation between the prediction error of a group and its model gradients. This relation is emphasized in Figure 3, which illustrates that the gradient norm for a given group increases as its prediction accuracy decreases.
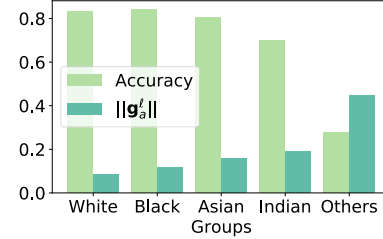
Proposition 2 allows us to link the gradient norms with the group accuracy of the resulting model, which, together with the result above will be useful to reason about the impact of gradient norms on the disparities in the group excessive losses.

The role of gradient norms in pruning. Having highlighted the connection between gradients norms of a group with the accuracy of the pruned model on such a group, this section provides theoretical intuitions on the role of gradient norms in the disparate group losses during pruning.

From Theorem 1, notice that the excessive loss is controlled by term $\|g_a^\ell\| \times \|\bar{\boldsymbol{\theta}} - \overset{\star}{\boldsymbol{\theta}}\|$. As already noted in Corollary 1, the term $\|\bar{\boldsymbol{\theta}} - \overset{\star}{\boldsymbol{\theta}}\|$ regulates the impact of pruning on the excessive loss, as the difference between the pruned and non-pruned parameters vectors directly depends on the pruning rate. For a fixed pruning rate, however, notice that groups with different gradient norms will have a disparate effect on the resulting term. In particular, groups with very small gradients norms (those generally associated with highly accurate predictions) will be less sensitive to the effects of the pruning rate. Conversely, groups with large gradient norms will be affected by the pruning rate to a greater extent, with larger pruning rates, *typically* reflecting in larger excessive losses.

These observations of the factors of disparity, accuracy, and group size, can also be appreciated empirically in Figures 4a and 4b. The plots report accuracy (a) and gradient norms (b) on the

5

UTKFace datasets for a variety of pruning rates. Consider group *White* (containing 42% of the total samples) and *Others* (containing 7% of the total samples). The unpruned model has high accuracy on the former group and small gradient norms. The accuracy of this group is insensitive to various pruning rates and even increases at large pruning regimes. In contrast, group *Others* has much lower accuracy and larger gradient norms in the unpruned model. As the pruning rate increase, their accuracies drastically drop. As a result, in high pruning regimes, this minority group exhibits poor accuracy and very high gradient norms.

Notice that the empirical results apply to much more complex settings than those which can be analyzed formally, thus they complement the theoretical observations.

5 Why disparity in groups' Hessians causes unfairness?

Having examined the properties of the groups gradients and their relation to unfairness in pruning, this section turns on analyzing how the Hessian associated with the loss function for a group is linked to the unfairness observed during pruning. In more detail, it connects the groups' Hessian to the distance to the decision boundary for the samples in that group and their resulting model errors (Theorem 2), it illustrates a strong positive correlation between groups' Hessian and gradient norms, and links these concepts with the excessive loss (Theorem 1) to show that unfairness in model pruning is controlled by the difference in maximum eigenvalues of the Hessians among groups.

Group Hessians and accuracy. The section first shows that groups presenting large Hessian values may suffer larger disparate impacts due to pruning, when compared with groups that have smaller Hessians. It does so by connecting the maximum eigenvalues of the groups Hessians with their distance to decision boundary and the group accuracy. The following result sheds light on these observations. It restricts its attention to models trained under binary cross entropy losses, for clarity of explanation, although an extension to a multi-class case is directly attainable.

Theorem 2. *Let f_θ be a binary classifier trained using a binary cross entropy loss. For any group $a \in \mathcal{A}$, the maximum eigenvalue of the group Hessian $\lambda(\boldsymbol{H}_a^\ell)$ can be upper bounded by:*

$$\lambda(\boldsymbol{H}_a^\ell) \leq \frac{1}{|D_a|} \sum_{(\boldsymbol{x},y)\in D_a} \underbrace{\left(f_{\hat{\boldsymbol{\theta}}}^\star(\boldsymbol{x})\right)\left(1 - f_{\hat{\boldsymbol{\theta}}}^\star(\boldsymbol{x})\right)}_{\text{Distance to decision boundary}} \times \left\|\nabla_{\boldsymbol{\theta}} f_{\hat{\boldsymbol{\theta}}}^\star(\boldsymbol{x})\right\|^2 + \underbrace{\left|f_{\hat{\boldsymbol{\theta}}}^\star(\boldsymbol{x}) - y\right|}_{\text{Accuracy}} \times \lambda\left(\nabla_{\boldsymbol{\theta}}^2 f_{\hat{\boldsymbol{\theta}}}^\star(\boldsymbol{x})\right). \quad (6)$$

The proof relies on derivations of the Hessian associated with model loss function and Weyl inequality. In other words, Theorem 2 highlights a direct connection between the maximum eigenvalue of the group Hessian and **(1)** the closeness to the decision boundary of the group samples, and **(2)** the accuracy of the group. The distance to the decision boundary is derived from [9]. Intuitively this term is maximized when the classifier is highly uncertain about the prediction: $f_{\hat{\boldsymbol{\theta}}}^\star(\boldsymbol{x}) \to 0.5$, and minimized when it is highly certain $f_{\hat{\boldsymbol{\theta}}}^\star(\boldsymbol{x}) \to 0$ or 1, as showed in the following proposition.

Proposition 3. *Consider a binary classifier $f_\theta(\boldsymbol{x})$. For a given sample $\boldsymbol{x} \in D$, the term $f_{\hat{\boldsymbol{\theta}}}^\star(\boldsymbol{x})(1 - f_{\hat{\boldsymbol{\theta}}}^\star(\boldsymbol{x}))$ is maximized when $f_{\hat{\boldsymbol{\theta}}}^\star(\boldsymbol{x}) = 0.5$ and minimized when $f_{\hat{\boldsymbol{\theta}}}^\star(\boldsymbol{x}) \in \{0, 1\}$.*

Observe that a group consisting of samples that are far from the decision boundary will have smaller Hessians and, thus, be less subject to a drop in accuracy due to model pruning. These results can be appreciated in Figure 5. Notice the inverse relationship between maximum eigenvalues of the groups' Hessians and their average distance to the decision boundary. The same relation also holds for accuracy: the higher the Hessians maximum eigenvalues, the smaller the accuracy. This is intuitive as samples which are close to the decision boundary will be more prone to errors due to small changes in the model due to pruning, when compared with samples lying far from the decision boundary.
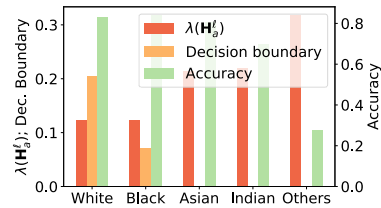

Figure 5: Group Hessians, distance to decision boundary, and accuracy.

Correlation between group Hessians and gradient norms. This section observes a positive correlation between maximum eigenvalues of the Hessian of a group and their gradient norms. This relation can be appreciated in Figure 6. While mainly empirical, this observation is important as it illustrates that both the Hessian $\lambda(\boldsymbol{H}_a^\ell)$ and the gradient $\|\boldsymbol{g}_a^\ell\|$ terms appearing in the upper bound of

the excessive loss $R(a)$ reported in Theorem 1 are in agreement. This relation was observed in all our experiments and settings. Such observation allows us to infer that it is the combined effect of gradient norms and group Hessians that is responsible for the excessive loss of a group and, in turn, for the exacerbation of unfairness in the pruned models.

The role of the group Hessian in pruning. Having highlighted the connection between Hessian for a group with the resulting accuracy of the model on such a group, this section provides theoretical intuitions on the role of the Hessians in the disparate group losses during pruning.

Figure 6: Group Hessians and gradient norms.

In Theorem 1, notice that the excessive loss is controlled by term $\|H_a^\ell\| \times \|\bar{\theta} - \overset{\star}{\theta}\|^2$. As also noted in the previous section, the term $\|\bar{\theta} - \overset{\star}{\theta}\|$ regulates the impact of pruning on the excessive loss as the difference between the pruned and non-pruned parameters vectors directly depends on the pruning rate. Similar to the observation for gradient norms, with a fixed pruning rate, groups with different Hessians will have a disparate effect on the resulting term. In particular, groups with small Hessians eigenvalues (those generally distant from the decision boundary and highly accurate) will be less sensitive to the effects of the pruning rate. Conversely, groups with large Hessians eigenvalues will be affected by the pruning rate to a greater extent, *typically* resulting in larger excessive losses. These observations can further be appreciated empirically in Figures 4a (for accuracy) and 4c (for maximum group Hessian eigenvalues) on the UTKFace datasets for a variety of pruning rates.
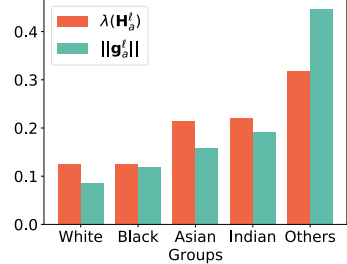
6 Mitigation solution and evaluation

The previous sections highlighted the presence of two key factors playing a role in the observed model accuracy disparities due to pruning: the difference in gradient norms, and the difference in Hessians losses across groups. This section first shows how to leverage these findings to provide a simple, yet effective solution to reduce the disparate impacts of pruning. Then, the section illustrates the benefits of this mitigating solution on a variety of tasks, datasets, and network architectures.

6.1 Mitigation solution

To achieve fairness, the aforementioned findings suggest to equalize the disparity associated with gradient norms $\|g_a^\ell\|$ and Hessians $\lambda(H_a^\ell)$ across different groups $a \in \mathcal{A}$. For this goal, the paper adopts a constrained empirical risk minimization approach:

$$\underset{\theta}{\text{minimize}} \quad J(\theta; D) \quad \text{such that: } \|g_a^\ell\| = \|g^\ell\|, \quad \lambda(H_a^\ell) = \lambda(H^\ell) \quad \forall a \in \mathcal{A}, \tag{7}$$

where $g^\ell = \nabla_\theta J(\theta; D)$ and $H^\ell = \nabla_\theta^2 J(\theta; D)$ refer to the gradients and Hessian associated with loss function ℓ, respectively, and are computed using the whole dataset D. The approach (7) is a common strategy adopted in fair learning tasks, and the paper uses the Lagrangian Dual method of Fioretto et al. [12] which exploits Lagrangian duality to extend the loss function with trainable and weighted regularization terms that encapsulate constraints violations (see Appendix C for additional details).

A shortcoming of this approach is, however, that requires computing the gradient norms and Hessian matrices of the group losses in each and every training iteration, rendering the process computationally unviable, especially for deep, overparametrized networks.

To overcome this computational burden, we will use two observations made earlier in the paper. First, recall the strong relation between gradient norms for a group and their associated losses. This aspect was noted in Proposition 2. That is, when the losses across the groups are similar, the gradient norms across such groups will also tend to be similar. Next, Theorem 2 noted a positive correlation between model errors (and thus loss values) for a group and its associated Hessian eigenvalues. Thus, when the losses across the groups are similar, the group Hessians will also tend to be similar. This intuition is also complemented by the strong correlation between group Hessians and gradient norms reported in Section 5. Based on the above observations, the paper proposes a simpler version of the constrained minimizer (7) defined as

$$\underset{\theta}{\text{minimize}} \quad J(\theta; D) \quad \text{such that: } J(\theta; D_a) = J(\theta; D) \quad \forall a \in \mathcal{A}, \tag{8}$$
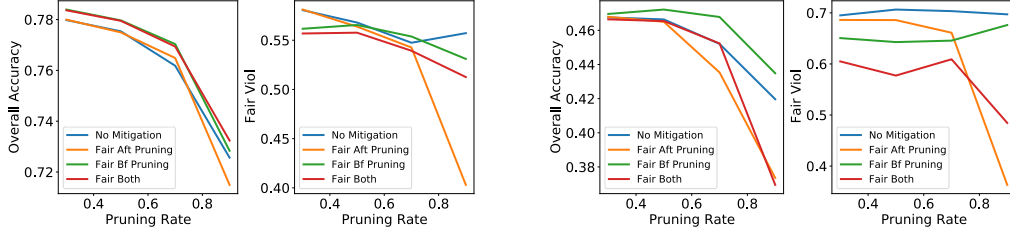
Figure 8: Accuracy and Fairness violations attained by all models on ResNet50, UTK-Face dataset with *ethnicity* (5 classes) as group attribute (and labels) [left] and *age* (9 classes) [right].
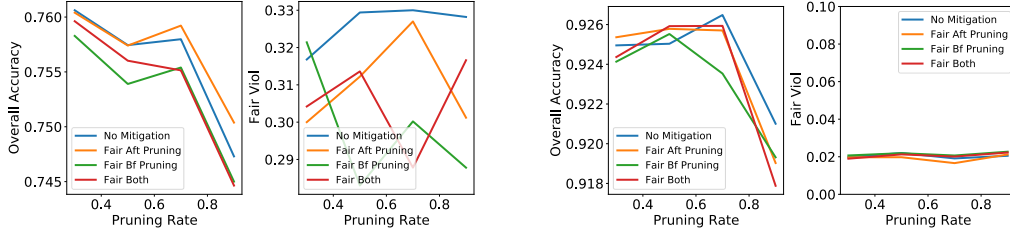

Figure 9: Accuracy and Fairness violations attained by all models on VGG-19, CIFAR-10 dataset (left) and SVHN (right) with 10 class labels also used as group attribute.

that substitutes the gradient norms and max eigenvalues of group Hessians equality constraints with proxy terms capturing the group $J(\theta; D_a)$ and population $J(\theta; D)$ losses.

The impact of such proxy terms in the fairness constrained program above can be appreciated, empirically, in Figure 7. The plots, that use the UTK-Face dataset, with Ethnicity as protected group, show an original unfair model (top) and a fair counterpart obtained through Program (8) (bottom). Notice how enforcing balance in the group losses also helps reducing and balancing the gradient norms and group's average distance to the decision boundary. As a consequence, the resulting model fairness is dramatically enhanced (bottom-left subplot).
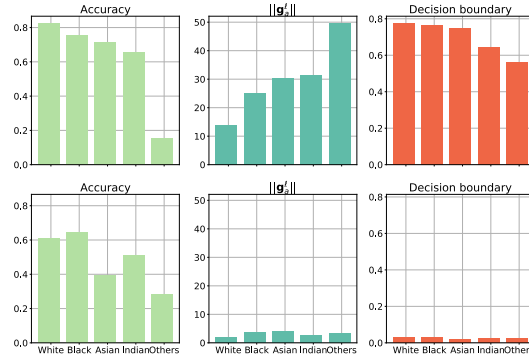

Figure 7: Effects of fairness constraints in balancing not only group accuracy (left) but also gradient norms (middle) and group average distance to the decision boundary (right).

6.2 Assessment of the mitigation solution

Datasets, models, and settings. This section analyzes the results obtained using the proposed mitigation solution with ResNet50 and VGG19 on the UTKFace dataset [39], CIFAR-10 [22], and SVHN [25] for various protected attributes. The experiments compare the following four models:

- *No Mitigation*: it refers to the standard pruning approach which uses no fairness mitigation strategy.
- *Fair Bf Pruning*: it applies the fairness mitigation process (Problem (8)) exclusively to the original large network, thus *before* pruning.
- *Fair Aft Pruning*: it applies the mitigation exclusively to the pruned network, thus *after* pruning.
- *Fair Both*: it applies the mitigation both to the original large network and to the pruned network.

The experiments report the overall accuracy of resulting models as well as their fairness violations, defined here as the difference between the maximal and minimal group accuracy. The reported metrics are the average of 10 repetitions. Additional details on datasets, architectures, hyper-parameters adopted, as well as additional and extended results are reported in Appendix C and C.

Effects on accuracy. The section first focuses on analyzing the effects of accuracy drop due to applying the proposed mitigation solution for fair pruning. Figure 8 compares the four models on the

8

UTK-Face dataset using a ResNet50 architecture. The left subplots use *ethnicity* as protected group and class label, with $|\mathcal{Y}| = 5$, while the right subplots use *age* as protected group and class label, with $|\mathcal{Y}| = 9$. Notice that, as expected, all compared models present some drop in accuracy as the pruning rates increase. However, notably, the accuracy drops of the models that apply the fair mitigation steps are comparable to (or even improved) those of the "*No mitigation*" model, which applies standard pruning.

A similar trend can be seen in Figure 9 that reports results on CIFAR (left) and SVHN (right). Both use the ten class labels as protected attributes. These results clearly illustrate the ability of the mitigating solution to preserve highly accurate models.

Effects on fairness. The section next illustrates the ability of the proposed solution to achieve fair pruned models. The second and fourth subplots presented in Figures 8 and 9 illustrate the fairness violations obtained by the four models analyzed on different datasets and settings. The paper makes the following observations: First, all the plots exhibit a consistent trend in that the mitigation solution produces models which improve the fairness of the baseline, "*No mitigation*" model. Observe that, as already illustrated in Figure 7, the fair models tend to equalize the gradient norms and group Hessians components (and thus the distance to the decision boundary across groups). Thus, the resulting pruned models also attain better fairness, when compared to their standard counterparts.

Next, notice that "*Fair Aft Pruning*" often achieves better fairness violations than "*Fair Bf Pruning*", especially at high pruning regimes. This is because the former has the advantage to apply the mitigation solution directly to the pruned model to ensure that the resulting model has low differences in gradient norms and group Hessians. The presentation also illustrates the application of the mitigation strategies both before and after pruning (*Fair Both*) which shows once again the significance of applying the mitigation solution over the pruned network.

Finally, it is notable that "*Fair Aft Pruning*" achieves good reductions in fairness violation. Indeed, pre-trained large (non-pruned) fair models may not be available and the ability to retrain these large models prior to pruning may be hindered by their size and complexity.

7 Discussion and limitations

This section discusses three key messages found in this study. First, we notice that pruning affecting model separability and distance to the decision boundary is related to concepts also explored in robust machine learning [14, 27]. Not surprisingly, some recent literature in network pruning has empirically observed that pruning may have a negative impact on adversarial robustness [15]. These observations raise questions about the connection between pruning, robustness, and fairness, which we believe is an important direction to further investigate.

Next, although the solution proposed in Problem (8) allows it to be adopted in large models, the size of modern ML models (together with the amount of hyperparameters searches) may hinder retraining such original massive models from incorporating fairness constraints. Notably, however, the proposed mitigation solution can be used as a post-processing step to be applied during the pruning operation directly. The previous section shows that the proposed method delivers desirable performance in terms of both accuracy and fairness.

Finally, we notice that the results analyzed in this paper pertain to losses that are twice differentiable. Lifting such an assumption will be an interesting and challenging future research avenue.

8 Conclusion

This work observed that pruning, while effective in compressing large models with minimal loss of accuracy, can result in substantial disparate accuracy impacts. The paper examined the factors causing such disparities both theoretically and empirically showing that: **(1)** disparity in gradient norms across groups and **(2)** disparity in Hessian matrices associated with the loss functions computed using a groups' data are two key factors responsible for such disparities to arise. By recognizing these factors, the paper also developed a simple yet effective retraining technique that largely mitigates the disparate impacts caused by pruning.

As reduced versions of large, overparametrized models become increasingly adopted in embedded systems to facilitate autonomous decisions, we believe that this work makes an important step toward *understanding* and *mitigating* the sources of disparate impacts observed in compressed learning models.

Acknowledgement

References

[1] N. Aghli and E. Ribeiro. Combining weight pruning and knowledge distillation for cnn compression. In *Proceedings of the IEEE/CVF Conference on Computer Vision and Pattern Recognition*, pages 3191–3198, 2021.

[2] O. Ahia, J. Kreutzer, and S. Hooker. The low-resource double bind: An empirical study of pruning for low-resource machine translation. In *EMNLP*, 2021.

[3] E. Bagdasaryan, O. Poursaeed, and V. Shmatikov. Differential privacy has disparate impact on model accuracy. In *Advances in Neural Information Processing Systems*, pages 15479–15488, 2019.

[4] S. Barocas, M. Hardt, and A. Narayanan. Fairness in machine learning. *Nips tutorial*, 1:2, 2017.

[5] C. Baykal, L. Liebenwein, I. Gilitschenski, D. Feldman, and D. Rus. Sipping neural networks: Sensitivity-informed provable pruning of neural networks. *arXiv preprint arXiv:1910.05422*, 2019.

[6] C. Blakeney, N. Huish, Y. Yan, and Z. Zong. Simon says: Evaluating and mitigating bias in pruned neural networks with knowledge distillation. *ArXiv*, abs/2106.07849, 2021.

[7] D. Blalock, J. J. G. Ortiz, J. Frankle, and J. Guttag. What is the state of neural network pruning? *arXiv preprint arXiv:2003.03033*, 2020.

[8] S. Caton and C. Haas. Fairness in machine learning: A survey. *arXiv preprint arXiv:2010.04053*, 2020.

[9] J. Cohen, E. Rosenfeld, and Z. Kolter. Certified adversarial robustness via randomized smoothing. In *International Conference on Machine Learning*, pages 1310–1320. PMLR, 2019.

[10] M. Du, S. Mukherjee, Y. Cheng, M. Shokouhi, X. Hu, and A. H. Awadallah. What do compressed large language models forget? robustness challenges in model compression. *ArXiv*, abs/2110.08419, 2021.

[11] C. Dwork, M. Hardt, T. Pitassi, O. Reingold, and R. Zemel. Fairness through awareness. In *Proceedings of the 3rd innovations in theoretical computer science conference*, pages 214–226, 2012.

[12] F. Fioretto, P. V. Hentenryck, T. W. Mak, C. Tran, F. Baldo, and M. Lombardi. Lagrangian duality for constrained deep learning. In *Joint European Conference on Machine Learning and Knowledge Discovery in Databases*, pages 118–135. Springer, 2020.

[13] F. Fioretto, C. Tran, P. V. Hentenryck, and K. Zhu. Differential privacy and fairness in decisions and learning tasks: A survey. *CoRR*, abs/2202.08187, 2022. URL https://arxiv.org/abs/2202.08187.

[14] I. J. Goodfellow, J. Shlens, and C. Szegedy. Explaining and harnessing adversarial examples, 2014. URL https://arxiv.org/abs/1412.6572.

[15] Y. Guo, C. Zhang, C. Zhang, and Y. Chen. Sparse dnns with improved adversarial robustness. In *Proceedings of the International Conference on Neural Information Processing Systems (NeurIPS)*, page 240–249, 2018.

[16] M. Hardt, E. Price, E. Price, and N. Srebro. Equality of opportunity in supervised learning. In D. Lee, M. Sugiyama, U. Luxburg, I. Guyon, and R. Garnett,

editors, *Advances in Neural Information Processing Systems*, volume 29. Curran Associates, Inc., 2016. URL https://proceedings.neurips.cc/paper/2016/file/9d2682367c3935defcb1f9e247a97c0d-Paper.pdf.

[17] K. He, X. Zhang, S. Ren, and J. Sun. Deep residual learning for image recognition. In *Proceedings of the IEEE conference on computer vision and pattern recognition*, pages 770–778, 2016.

[18] S. Hooker, A. C. Courville, G. Clark, Y. Dauphin, and A. Frome. What do compressed deep neural networks forget. *arXiv: Learning*, 2020.

[19] S. Hooker, N. Moorosi, G. Clark, S. Bengio, and E. L. Denton. Characterising bias in compressed models. *ArXiv*, abs/2010.03058, 2020.

[20] S. Hosseini, M. A. Shabani, M. M. Jahanara, and B. Salamatian. Learning fair from unfair teachers.

[21] V. Joseph, S. A. Siddiqui, A. Bhaskara, G. Gopalakrishnan, S. Muralidharan, M. Garland, S. Ahmed, and A. R. Dengel. Going beyond classification accuracy metrics in model compression. 2020.

[22] A. Krizhevsky, V. Nair, and G. Hinton. Cifar-10 (canadian institute for advanced research). URL http://www.cs.toronto.edu/~kriz/cifar.html.

[23] N. Mehrabi, F. Morstatter, N. Saxena, K. Lerman, and A. Galstyan. A survey on bias and fairness in machine learning. *ACM Computing Surveys (CSUR)*, 54(6):1–35, 2021.

[24] M. C. Mozer and P. Smolensky. Skeletonization: A technique for trimming the fat from a network via relevance assessment. In D. Touretzky, editor, *Advances in Neural Information Processing Systems*, volume 1. Morgan-Kaufmann, 1988. URL https://proceedings.neurips.cc/paper/1988/file/07e1cd7dca89a1678042477183b7ac3f-Paper.pdf.

[25] Y. Netzer, T. Wang, A. Coates, A. Bissacco, B. Wu, and A. Ng. Reading digits in natural images with unsupervised feature learning. 2011.

[26] M. Paganini. Prune responsibly. *arXiv preprint arXiv:2009.09936*, 2020.

[27] N. Papernot, P. McDaniel, and I. Goodfellow. Transferability in machine learning: from phenomena to black-box attacks using adversarial samples. *arXiv preprint arXiv: Arxiv-1605.07277*, 2016.

[28] D. Pujol, R. McKenna, S. Kuppam, M. Hay, A. Machanavajjhala, and G. Miklau. Fair decision making using privacy-protected data. In *Proceedings of the 2020 Conference on Fairness, Accountability, and Transparency*, pages 189–199, 2020.

[29] A. Renda, J. Frankle, and M. Carbin. Comparing rewinding and fine-tuning in neural network pruning. In *International Conference on Learning Representations*, 2020. URL https://openreview.net/forum?id=S1gSj0NKvB.

[30] J. T. S. Han, J. Pool and W. J. Dally. Learning both weights and connections for efficient neural networks. In *NIPS*, 2015. URL https://arxiv.org/abs/1506.02626v3.

[31] V. Sehwag, S. Wang, P. Mittal, and S. Jana. Towards compact and robust deep neural networks. *preprint arXiv:1906.06110*, 2019.

[32] W. Toussaint, A. Mathur, F. Kawsar, and A. Y. Ding. Tiny, always-on and fragile: Bias propagation through design choices in on-device machine learning workflows, 2022. URL https://arxiv.org/abs/2201.07677.

[33] C. Tran, M. Dinh, and F. Fioretto. Differentially private empirical risk minimization under the fairness lens. In *Advances in Neural Information Processing Systems*, 2021.

[34] C. Tran, F. Fioretto, P. V. Hentenryck, and Z. Yao. Decision making with differential privacy under a fairness lens. In Z. Zhou, editor, *International Joint Conference on Artificial Intelligence (IJCAI)*, pages 560–566, 2021.

[35] A. Uniyal, R. Naidu, S. Kotti, S. Singh, P. J. Kenfack, F. Mireshghallah, and A. Trask. Dp-sgd vs pate: Which has less disparate impact on model accuracy? *ArXiv*, abs/2106.12576, 2021.

[36] C. Xu, W. Zhou, T. Ge, K. Xu, J. McAuley, and F. Wei. Beyond preserved accuracy: Evaluating loyalty and robustness of BERT compression. In *Proceedings of the 2021 Conference on Empirical Methods in Natural Language Processing*, pages 10653–10659, Online and Punta

Cana, Dominican Republic, Nov. 2021. Association for Computational Linguistics. doi: 10. 18653/v1/2021.emnlp-main.832. URL https://aclanthology.org/2021.emnlp-main. 832.

[37] G. Xu and Q. Hu. Can model compression improve nlp fairness. *ArXiv*, abs/2201.08542, 2022.

[38] H. Xu, X. Liu, Y. Li, A. K. Jain, and J. Tang. To be robust or to be fair: Towards fairness in adversarial training, 2021.

[39] S. Y. Zhang, Zhifei and H. Qi. Age progression/regression by conditional adversarial autoencoder. In *IEEE Conference on Computer Vision and Pattern Recognition (CVPR)*. IEEE, 2017.

[40] T. Zhang, S. Ye, K. Zhang, J. Tang, W. Wen, M. Fardad, and Y. Wang. A systematic dnn weight pruning framework using alternating direction method of multipliers. In *Proceedings of the European Conference on Computer Vision (ECCV)*, pages 184–199, 2018.

[41] H. Zhao and G. Gordon. Inherent tradeoffs in learning fair representations. *Advances in neural information processing systems*, 32:15675–15685, 2019.

[42] K. Zhu, P. Van Hentenryck, and F. Fioretto. Bias and variance of post-processing in differential privacy. In *Proceedings of the AAAI Conference on Artificial Intelligence*, pages 11177–11184, 2021.

[43] Z. Zhu, T. Luo, and Y. Liu. The rich get richer: Disparate impact of semi-supervised learning. *arXiv preprint arXiv:2110.06282*, 2021.

A Missing Proofs

Theorem 1. *The excessive loss of a group $a \in \mathcal{A}$ is upper bounded by*[2]:

$$R(a) \le \left\| g_a^\ell \right\| \times \left\| \bar{\theta} - \mathring{\theta} \right\| + \frac{1}{2}\lambda\left(H_a^\ell \right) \times \left\| \bar{\theta} - \mathring{\theta} \right\|^2 + O\left(\left\| \bar{\theta} - \mathring{\theta} \right\|^3 \right), \tag{9}$$

where $g_a^\ell = \nabla_{\mathring{\theta}} J(\mathring{\theta}; D_a)$ is the vector of gradients associated with the loss function ℓ evaluated at $\mathring{\theta}$ and computed using group data D_a, $H_a^\ell = \nabla_{\mathring{\theta}}^2 J(\mathring{\theta}; D_a)$ is the Hessian matrix of the loss function ℓ, at the optimal parameters vector $\mathring{\theta}$, computed using the group data D_a (henceforth simply referred to as group hessian), and $\lambda(\Sigma)$ is the maximum eigenvalue of a matrix Σ.

Proof. Using a second order Taylor expansion around $\mathring{\theta}$, the excessive loss $R(a)$ for a group $a \in \mathcal{A}$ can be stated as:

$$R(a) = J(\bar{\theta}; D_a) - J(\mathring{\theta}; D_a)$$
$$= \left[J\left(\mathring{\theta}; D_a\right) + \left(\bar{\theta} - \mathring{\theta}\right)^\top \nabla_\theta J\left(\mathring{\theta}; D_a\right) + \frac{1}{2}\left(\bar{\theta} - \mathring{\theta}\right)^\top H_a^\ell \left(\bar{\theta} - \mathring{\theta}\right) + O\left(\left\| \mathring{\theta} - \bar{\theta} \right\|^3 \right) \right] - J\left(\mathring{\theta}; D_a\right)$$
$$= \left(\bar{\theta} - \mathring{\theta}\right)^\top g_a^\ell + \frac{1}{2}\left(\bar{\theta} - \mathring{\theta}\right)^\top H_a^\ell \left(\bar{\theta} - \mathring{\theta}\right) + O\left(\left\| \mathring{\theta} - \bar{\theta} \right\|^3 \right)$$

The above, follows from the loss $\ell(\cdot)$ being at least twice differentiable, by assumption.

By Cauchy-Schwarz inequality, it follows that

$$\left(\bar{\theta} - \mathring{\theta}\right)^\top g_a^\ell \le \left\| \bar{\theta} - \mathring{\theta} \right\| \times \left\| g_a^\ell \right\|.$$

In addition, due to the property of Rayleigh quotient we have:

$$\frac{1}{2}\left(\bar{\theta} - \mathring{\theta}\right)^\top H_a^\ell \left(\bar{\theta} - \mathring{\theta}\right) \le \frac{1}{2}\lambda\left(H_a^\ell \right) \times \left\| \bar{\theta} - \mathring{\theta} \right\|^2.$$

The upper bound for the excessive loss $R(a)$ is thus obtained by combining these two inequalities. $\square$

Proposition 1. *Consider two groups a and b in $\mathcal{A}$ with $|D_a| \ge |D_b|$. Then $\left\| g_a^\ell \right\| \le \left\| g_b^\ell \right\|$.*

Proof. By the assumption that the model converges to a local minima, it follows that:

$$\nabla_\theta \mathcal{L}(\mathring{\theta}; D) = \sum_{a \in \mathcal{A}} \frac{|D_a|}{|D|} \nabla_\theta J(\mathring{\theta}; D_a)$$
$$= \frac{|D_a|}{|D|} g_a^\ell + \frac{|D_b|}{|D|} g_b^\ell = 0$$

Thus, $g_a^\ell = -\frac{|D_b|}{|D_a|} g_b$. Hence $\|g_a^\ell\| = \frac{|D_b|}{|D_a|}\|g_b^\ell\| \le \|g_b^\ell\|$, because $|D_a| \ge |D_b|$. $\square$

Proposition 2. *For a given group $a \in \mathcal{A}$, gradient norms can be upper bounded as:*

$$\|g_a^\ell\| \in O\left(\sum_{(\boldsymbol{x},y)\in D_a} \underbrace{\|f_{\mathring{\theta}}(\boldsymbol{x}) - y\|}_{Accuracy} \times \left\| \nabla_{\mathring{\theta}} f_{\mathring{\theta}}(\boldsymbol{x}) \right\| \right).$$

The above proposition is presented in the context of cross entropy loss or mean squared error loss functions. These two cases are reviewed as follows

---

[2]With a slight abuse of notation, the results refer to $\bar{\theta}$ as the homonymous vector which is extended with $k - \bar{k}$ zeros.

Cross Entropy Loss. Consider a classification task with cross entropy loss: $\ell(f_{\hat{\theta}}(\boldsymbol{x}), y) = -\sum_{z \in \mathcal{Y}} f_{\hat{\theta}}^z(\boldsymbol{x})\boldsymbol{y}^z$, where $f_{\hat{\theta}}^z(\boldsymbol{x})$ represents the z-th element of the output associated with the softmax layer of model $f_{\hat{\theta}}$, and $\boldsymbol{y}$ is a one-hot encoding of the true label y, with $\boldsymbol{y}^z$ representing its z-th element, then,

$$\|\boldsymbol{g}_a\| = \left\|\nabla_{\boldsymbol{\theta}} J(\hat{\boldsymbol{\theta}}; D_a,)\right\| = \left\|{}^{1\!}/{}_{|D_a|} \sum_{(\boldsymbol{x},y) \in D_a} \nabla_f \ell(f_{\hat{\theta}}(\boldsymbol{x}), y) \times \nabla_{\boldsymbol{\theta}} f_{\hat{\theta}}(\boldsymbol{x})\right\|$$

$$= \left\|{}^{1\!}/{}_{|D_a|} \sum_{(\boldsymbol{x},y) \in D_a} (f_{\hat{\theta}}(\boldsymbol{x}) - \boldsymbol{y}) \times \nabla_{\boldsymbol{\theta}} f_{\hat{\theta}}(\boldsymbol{x})\right\|$$

$$\leq {}^{1\!}/{}_{|D_a|} \sum_{(\boldsymbol{x},y) \in D_a} \left\|f_{\hat{\theta}}(\boldsymbol{x}) - \boldsymbol{y}\right\| \times \left\|\nabla_{\boldsymbol{\theta}} f_{\hat{\theta}}(\boldsymbol{x})\right\|,$$

where the third equality is due to that the gradient of the cross entropy loss reduces to $f_{\hat{\theta}}(\boldsymbol{x}) - \boldsymbol{y}$.

Mean Squared Error. Next, consider a regression task with mean squared error loss $\ell(f_{\hat{\theta}}(\boldsymbol{x}), y) = (f_{\hat{\theta}}(\boldsymbol{x}) - y)^2$. Using the same notation as that made above, if follows:

$$\|\boldsymbol{g}_a\| = \left\|\nabla_{\boldsymbol{\theta}} J(\hat{\boldsymbol{\theta}}; D_a,)\right\| = \left\|{}^{1\!}/{}_{|D_a|} \sum_{(\boldsymbol{x},y) \in D_a} \nabla_f \ell(f_{\hat{\theta}}(\boldsymbol{x}), y) \times \nabla_{\boldsymbol{\theta}} f_{\hat{\theta}}(\boldsymbol{x})\right\|$$

$$= \left\|{}^{2\!}/{}_{|D_a|} \sum_{(\boldsymbol{x},y) \in D_a} (f_{\hat{\theta}}(\boldsymbol{x}) - \boldsymbol{y}) \times \nabla_{\boldsymbol{\theta}} f_{\hat{\theta}}(\boldsymbol{x})\right\|$$

$$\leq {}^{2\!}/{}_{|D_a|} \sum_{(\boldsymbol{x},y) \in D_a} \left\|f_{\hat{\theta}}(\boldsymbol{x}) - \boldsymbol{y}\right\| \times \left\|\nabla_{\boldsymbol{\theta}} f_{\hat{\theta}}(\boldsymbol{x})\right\|,$$

where the third equality is due to that the gradient of the mean squared error loss w.r.t. $f_{\hat{\theta}}(\cdot)$ reduces to $2(f_{\hat{\theta}}(\boldsymbol{x}) - \boldsymbol{y})$.

Theorem 2. *Let f_{θ} be a binary classifier trained using a binary cross entropy loss. For any group $a \in \mathcal{A}$, the maximum eigenvalue of the group Hessian $\lambda(\boldsymbol{H}_a^{\ell})$ can be upper bounded by:*

$$\lambda(\boldsymbol{H}_a^{\ell}) \leq \frac{1}{|D_a|} \sum_{(\boldsymbol{x},y) \in D_a} \underbrace{\left(f_{\hat{\theta}}(\boldsymbol{x})\right)\left(1 - f_{\hat{\theta}}(\boldsymbol{x})\right)}_{\text{Distance to decision boundary}} \times \left\|\nabla_{\boldsymbol{\theta}} f_{\hat{\theta}}(\boldsymbol{x})\right\|^2 + \underbrace{\left|f_{\hat{\theta}}(\boldsymbol{x}) - y\right|}_{\text{Accuracy}} \times \lambda\left(\nabla_{\boldsymbol{\theta}}^2 f_{\hat{\theta}}(\boldsymbol{x})\right). \qquad (10)$$

Proof. First notice that an upper bound for the Hessian loss computed on a group $a \in \mathcal{A}$ can be derived as:

$$\lambda(\boldsymbol{H}_a^{\ell}) = \lambda\left(\frac{1}{|D_a|} \sum_{(\boldsymbol{x},y) \in D_a} \boldsymbol{H}_{\boldsymbol{x}}^{\ell}\right) \leq \frac{1}{|D_a|} \sum_{(\boldsymbol{x},y) \in D_a} \lambda\left(\boldsymbol{H}_{\boldsymbol{x}}^{\ell}\right) \qquad (11)$$

where $\boldsymbol{H}_{\boldsymbol{x}}^{\ell}$ represents the Hessian loss associated with a sample $\boldsymbol{x} \in D_a$ from group a. The above follows Weily's inequality which states that for any two symmetric matrices A and B, $\lambda(A + B) \leq \lambda(A) + \lambda(B)$.

Next, we will derive an upper bound on the Hessian loss associated to a sample $\boldsymbol{x}$. First, based on the chain rule a closed form expression for the Hessian loss associated to a sample $\boldsymbol{x}$ can be written as follows:

$$\boldsymbol{H}_{\boldsymbol{x}}^{\ell} = \nabla_f^2 \ell\left(f_{\hat{\theta}}(\boldsymbol{x}), y\right)\left[\nabla_{\boldsymbol{\theta}} f_{\hat{\theta}}(\boldsymbol{x})\left(\nabla_{\boldsymbol{\theta}} f_{\hat{\theta}}(\boldsymbol{x})\right)^{\top}\right] + \nabla_f \ell\left(f_{\hat{\theta}}(\boldsymbol{x}), y\right)\nabla_{\boldsymbol{\theta}}^2 f_{\hat{\theta}}(\boldsymbol{x}). \qquad (12)$$

The next follows from that

$$\nabla_f \ell\left(f_{\hat{\theta}}(\boldsymbol{x}), y\right) = (f_{\hat{\theta}}(\boldsymbol{x}) - y),$$

$$\nabla_f^2 \ell\left(f_{\hat{\theta}}(\boldsymbol{x}), y\right) = f_{\hat{\theta}}(\boldsymbol{x})\left(1 - f_{\hat{\theta}}(\boldsymbol{x})\right).$$

14

Applying the Weily inequality again on the R.H.S. of Equation 12, we obtain:

$$\lambda(\boldsymbol{H}_{\boldsymbol{x}}^{\ell}) \le f_{\hat{\boldsymbol{\theta}}}(\boldsymbol{x})\left(1 - f_{\hat{\boldsymbol{\theta}}}(\boldsymbol{x})\right) \times \left\|\nabla_{\boldsymbol{\theta}} f_{\hat{\boldsymbol{\theta}}}(\boldsymbol{x})\right\|^2 + \lambda\left(f_{\hat{\boldsymbol{\theta}}}(\boldsymbol{x}) - y\right) \times \nabla_{\boldsymbol{\theta}}^2 f_{\hat{\boldsymbol{\theta}}}(\boldsymbol{x})$$

$$\le f_{\hat{\boldsymbol{\theta}}}(\boldsymbol{x})\left(1 - f_{\hat{\boldsymbol{\theta}}}(\boldsymbol{x})\right) \times \left\|\nabla_{\boldsymbol{\theta}} f_{\hat{\boldsymbol{\theta}}}(\boldsymbol{x})\right\|^2 + \left|f_{\hat{\boldsymbol{\theta}}}(\boldsymbol{x}) - y\right| \lambda\left(\nabla_{\boldsymbol{\theta}}^2 f_{\hat{\boldsymbol{\theta}}}(\boldsymbol{x})\right) \tag{13}$$

The statement of Theorem 2 is obtained combining Equations 13 with 11. □

Proposition 3. *Consider a binary classifier $f_{\boldsymbol{\theta}}(\boldsymbol{x})$. For a given sample $\boldsymbol{x} \in D$, the term $f_{\hat{\boldsymbol{\theta}}}^\star(\boldsymbol{x})(1 - f_{\hat{\boldsymbol{\theta}}}^\star(\boldsymbol{x}))$ is maximized when $f_{\hat{\boldsymbol{\theta}}}^\star(\boldsymbol{x}) = 0.5$ and minimized when $f_{\hat{\boldsymbol{\theta}}}^\star(\boldsymbol{x}) \in \{0, 1\}$.*

Proof. First, notice that $f_{\hat{\boldsymbol{\theta}}}^\star(\boldsymbol{x}) \in [0, 1]$, as it represents the soft prediction (that returned by the last layer of the network), thus $f_{\hat{\boldsymbol{\theta}}}^\star(\boldsymbol{x}) \ge f_{\hat{\boldsymbol{x}}}^2(\boldsymbol{x})$. It follows that:

$$f_{\hat{\boldsymbol{\theta}}}^\star(\boldsymbol{x})\left(1 - f_{\hat{\boldsymbol{\theta}}}^\star(\boldsymbol{x})\right) = f_{\hat{\boldsymbol{\theta}}}^\star(\boldsymbol{x}) - f_{\hat{\boldsymbol{\theta}}}^2(\boldsymbol{x}) \ge 0. \tag{14}$$

In the above, it is easy to observe that the equality holds when either $f_{\hat{\boldsymbol{\theta}}}^\star(\boldsymbol{x}) = 0$ or $f_{\hat{\boldsymbol{\theta}}}^\star(\boldsymbol{x}) = 1$.

Next, by the Jensen inequality, it follows that:

$$f_{\hat{\boldsymbol{\theta}}}^\star(\boldsymbol{x})\left(1 - f_{\hat{\boldsymbol{\theta}}}^\star(\boldsymbol{x})\right) \le \frac{\left(f_{\hat{\boldsymbol{\theta}}}^\star(\boldsymbol{x}) + 1 - f_{\hat{\boldsymbol{\theta}}}^\star(\boldsymbol{x})\right)^2}{4} = \frac{1}{4}. \tag{15}$$

The above holds when $f_{\hat{\boldsymbol{\theta}}}^\star(\boldsymbol{x}) = 1 - f_{\hat{\boldsymbol{\theta}}}^\star(\boldsymbol{x})$, in other words, when $f_{\hat{\boldsymbol{\theta}}}^\star(\boldsymbol{x}) = 0.5$. Notice that, in the case of binary classifier, this refers to the case when the sample $\boldsymbol{x}$ lies on the decision boundary. □

B Dataset and Experimental Settings

B.1 Datasets

The paper uses the following datasets to validate the findings discussed in the main paper:

- **UTK-Face** [39]. A large-scale face dataset with a long age span (range from 0 to 116 years old). The dataset consists of over 20,000 face images with annotations of age, gender, and ethnicity. The images cover large variations in pose, facial expression, illumination, occlusion, resolution, etc. The experiments adopt the following attributes for classification (e.g., $\mathcal{Y}$) and as protected group ($\mathcal{A}$): *ethnicity, age bins, gender*.

- **CIFAR-10** [22]. This dataset consists of 60,000 32×32 RGB images in 10 classes, with 6,000 images per class. The 10 different classes represent airplanes, cars, birds, cats, deer, dogs, frogs, horses, ships, and trucks.

- **SVHN** [25] Street View House Numbers (SVHN) is a digit classification dataset that contains 600,000 32×32 RGB images of printed digits (from 0 to 9) cropped from pictures of house number plates.

B.2 Architectures, Hyper-parameters, and Settings

The study adopts the following architectures to validate the results of the main paper:

- **ResNet18**: An 18-layer architecture, with 8 residual blocks. Each residual block consists of two convolution layers. The model has $\sim$ 11 million trainable parameters.

- **ResNet50** This model contains 48 convolution layers, 1 MaxPool layer and a AvgPool layer. ResNet50 has $\sim$ 25 million trainable parameters.

- **VGG-19** This model consists of 19 layers (16 convolution layers, 3 fully connected layers, 5 MaxPool layers and 1 SoftMax layer). The model has $\sim$ 143 million parameters.

Hyperparameters for each of the above models was performed over a grid search (for different learning rates = $[0.0001, 0.001, 0.01, 0.1, 0.5, 0.05, 0.005, 0.0005]$) over a cluster of NVIDIA RTX A6000 with the above networks using the UTKFace dataset. The models with the highest accuracy
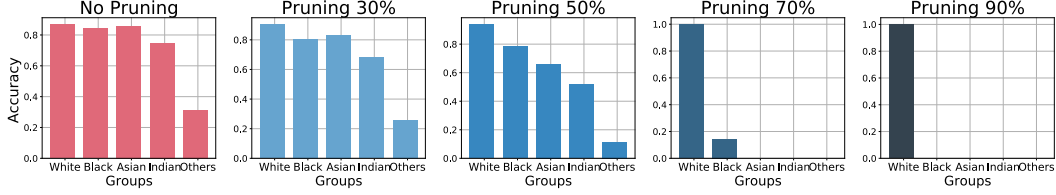
Figure 10: Accuracy of each demographic group in the UTK-Face dataset with ethnicity (5 classes) as group attribute using VGG19 over increasing pruning rates.
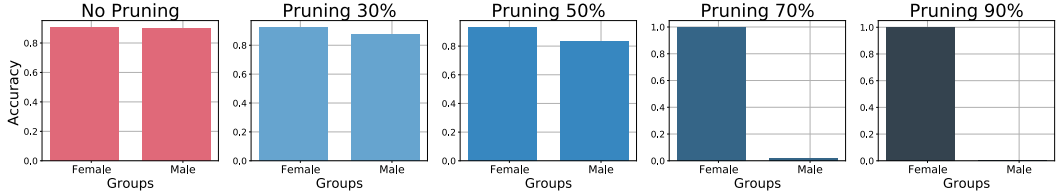

Figure 11: Accuracy of each demographic group in the UTK-Face dataset with gender (2 classes) as group attribute using VGG19 over increasing pruning rates.

were chosen and employed for the assessment of the mitigation solution in Sec. 6.2. The running time required for all sets of experiments which include mitigation solutions was about ~3 *days*.

The training uses the SGD optimizer with a momentum of 0.9 and weight_decay of $1e^{-4}$. Finally, the Lagrangian step size adopted in the Lagrangian dual learning framework [12] is set to 0.001.

All the models developed were implemented using Pytorch 3.0. The training was performed using NVidia Tesla P100-PCIE-16GB GPUs and 2GHz Intel Cores. The model was run for 100 epochs for the CIFAR-10 and SVHN and 40 epochs for UTK-Face dataset. Each reported experiment is an average of 10 repetitions. In all experiments, the protected group set coincides with the target label set: i.e., $\mathcal{A} = \mathcal{Y}$.

C   Additional Experimental Results

C.1   Impact of pruning on fairness

This section shows and affirms the impact of pruning towards accuracy disparity through VGG-19 network. The same training procedures as employed with ResNet18 in Fig 1 were followed. Each demographic group's accuracy is shown before and after pruning on the UTK-Face dataset in two cases: when *ethnicity* is a group attribute as in Figure 10, and when *gender* is a group attribute as in Figure 11. A consistent message is that under a higher pruning rate, the accuracies are more imbalanced across different groups, emphasizing the negative impact of pruning on fairness.

C.2   Correlation of gradient/hessian norm and average distance to the decision boundary

This subsection elaborates the impact of gradient norms and group Hessians towards the fairness issues shown in Figures 10 and 11. In Section 4, it has been shown that the group with a larger gradient norm before pruning will be penalized more than the groups with a smaller gradient norm. Figures 13 and 12 show the gradient norm of each demographic group for UTK-Face dataset under two choices of protected attributes for VGG 19 networks. The results indicate that a group penalized less will have a smaller gradient norm with respect to those of the other groups.

In addition, Section 5 supports that Hessian norm is another factor. More precisely, the groups with a larger Hessian norm will be penalized more (drop much more in accuracy) than groups with a smaller Hessian norm. Evidence is provided for the claim on VGG19 in Figures 12 and 13. These results on VGG19 again confirm the theoretical findings.

Finally, in Section 5, a positive correlation between gradient norms and Hessian groups is shown in Theorem 2, and a negative correlation between Hessian groups and distance to the decision boundary
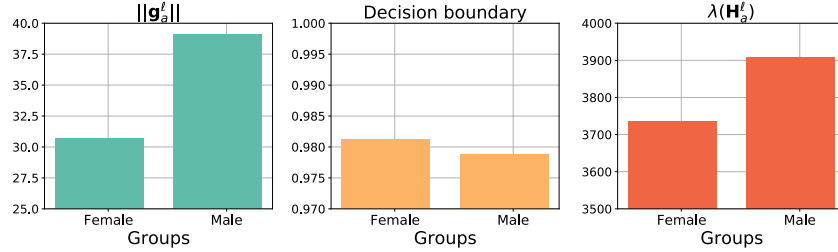
Figure 12: Gradient/Hessian norm and average distance to the decision boundary of each demographic group in the UTK-Face dataset with gender (2 classes) as group attribute using VGG19 with no pruning.
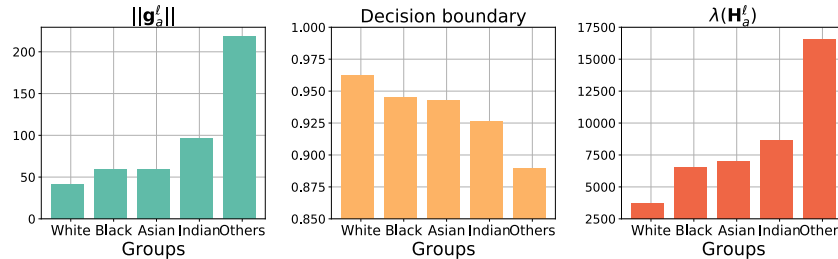

Figure 13: Gradient/Hessian norm and average distance to the decision boundary of each demographic group in the UTK-Face dataset with ethnicity (5 classes) as group attribute using VGG19 with no pruning.

is shown in Proposition 3. These important results again are supported by the results in Figures 12 and 13.

C.3 Impact of group sizes to gradient norm

This section presents additional empirical results to support Theorem 1, stating that the group with more samples will tend to have a smaller gradient norm. In these experiments, run on a ResNet50 network, one group is chosen and upsampled $1\times$, $5\times$, $10\times$, and $20\times$ times. Note that by increasingly upsampling it, the group becomes the majority group in that dataset. A group with *more samples* is expected to end up with a *smaller gradient norm* when the training convergences.

UTK-Face with gender   Since the UTK-Face is balanced with regard to gender (Female/Male), the number of samples in Female, and Male groups is upsampled in turn. Figure 14 reports the respective gradient norms at the last training iteration when upsampling Females (left) and Males (right.) Note how the Male group, initially with no upsampling, has a larger gradient norm than the Female group (right sub-plot). However, if the number of Male samples is increased enough, its gradient norm becomes smaller than that of the Female group.

UTK-Face with age bins   Similar experiments are performed with UTK-Face on nine age bin groups. Three age bins are randomly chosen, 0, 2, 4, and the number of samples for each group is upsampled in turn. The gradient norms of nine age bin groups are shown in Figure 15, where the upsampled groups are highlighted with dotted thick lines. The results echo that if a group's number of samples is increased enough, its gradient norm at convergence will be smaller than the other 8 age bin groups.
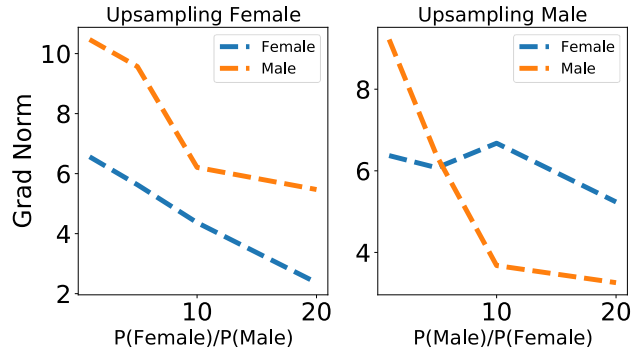
Figure 14: Impact of group sizes to the gradient norm per group in UTK-Face datase where groups are Male and Female.
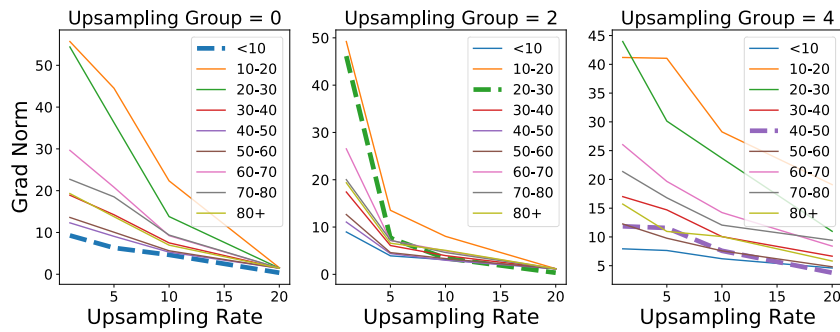

Figure 15: Impact of group sizes to the gradient norm per group in UTK-Face dataset where groups are nine age bins. The group with dotted thick line is a *majority group* in each chart.